Received August 24, 2017, accepted October 15, 2017, date of publication October 30, 2017, date of current version December 5, 2017.

Digital Object Identifier 10.1109/ACCESS.2017.2767618

An Innovative Hybrid Wind-Solar and Battery-Supercapacitor Microgrid System–Development and Optimization

UMER AKRAM, (Student Member, IEEE), MUHAMMAD KHALID, (Member, IEEE), AND SAIFULLAH SHAFIQ

Electrical Engineering Department, King Fahd University of Petroleum and Minerals, Dhahran 31261, Saudi Arabia

Corresponding author: Umer Akram (g201512930@kfupm.edu.sa)

This work was supported by the Deanship of Research at the King Fahd University of Petroleum and Minerals under Project SR161001.

ABSTRACT This paper presents a methodology for the joint capacity optimization of renewable energy (RE) sources, i.e., wind and solar, and the state-of-the-art hybrid energy storage system (HESS) comprised of battery energy storage (BES) and supercapacitor (SC) storage technology, employed in a grid-connected microgrid (MG). The problem involves multiple fields, i.e., RE, battery technology, SC technology, and control theory, and requires an efficient and precise co-ordination between sub-fields to harness the full benefits, making the problem labyrinthine. The optimization problem is formulated, and it involves a variety of realistic constraints from both hybrid generation and storage, and an objective function is proposed to: 1) minimize the cost; 2) improve the reliability; and 3) curtail greenhouse gases (GHG) emissions. The complex optimization problem is solved innovatively in piecewise fashion to decrease the complexity and computational time. First, sizes of solar photovoltaic (PV) and wind turbine (WT) are determined using an innovative search algorithm, and in the second step, the size of HESS is calculated, finally the optimal solution is determined. A comparison based upon cost, reliability, and GHG emissions is presented which plainly shows the effectiveness of the proposed methodology. The technique is also applied to determine the size of an MG employing PV, WT, and BES operating in grid-connected mode. And a brief cost analysis, reliability assessment, and emission reduction are given for three scenarios: 1) MG with HESS; 2) MG with BES; and 3) MG with conventional generation. It is shown that an MG with HESS is not only economical but also more reliable and has lower GHG emissions.

INDEX TERMS Hybrid energy storage, microgrid, optimization, renewable power.

NOMENCLATURE

A. ABBREVIATIONS

BES	Battery energy storage
DG	Distributed generator
ERBC	Emission reduction benefit cost
ESS	Energy storage system
GHG	Greenhouse gases
HESS	Hybrid energy storage system
MG	Microgrid
PSO	Particle swarm optimization
PV	Photovoltaic
RE	Renewable energy
SC	Supercapacitor
UG	Utility grid
WT	Wind turbine

B. INDICES

i	Index of PV
j	Index of WT
t	Time
u	Case number
w	Iteration number

C. PARAMETERS

A	Area of PV array
B_{lim}	Minimum battery utilization limit
c	Scale factor
e	Allowable tolerance
FOR_{PV}	Forced outage rate of PV
FOR_{WT}	Forced outage rate of WT
I	Solar irradiation

n	Total number of intervals
N	Total number of renewable sources types
N_{PV}	Number of PVs
N_{WT}	Number of WTs
P_{rated}	Rated power of WT
T_o	Atmospheric temperature
v_r	Rated speed of WT
v_{ci}	Cut-in speed of WT
v_{co}	Cut-out speed of WT
η_{PV}	Efficiency of PV
η_c	Charging efficiency of battery
η_d	Discharging efficiency of battery
η	Efficiency of supercapacitor
ξ	Self discharge rate of supercapacitor
Δt	Time step
σ	Shape factor

D. VARIABLES

B_{max}	Maximum energy capacity of battery
B_{cap}	Required energy capacity of battery
B_{opt}	Optimal energy capacity of battery
B_{chg}	Battery charging factor
BCS	Battery corrected size
BDV	Battery decision variable
C_{max}	Maximum energy capacity of supercapacitor
C_{cap}	Required energy capacity of supercapacitor
C_{opt}	Optimal energy capacity of supercapacitor
C_{inv-sc}	Investment cost of renewable energy sources
$C_{c,sr}$	Capital cost of renewable energy sources
$C_{inv-stg}$	Investment cost of storage
$C_{c,stg}$	Capital cost of storage
$C_{rep-stg}$	Replacement cost of storage
C_{om}	Operation and maintenance cost
$C_{om,f}$	Fixed operation and maintenance cost
$C_{om,v}$	Variable operation and maintenance cost
C_{MG-U}	Total cost of energy supplied by MG to UG
C_{U-MG}	Total cost of energy supplied by UG to MG
C_{exchg}	Per-unit cost of the exchanged power
C_{ERBC}	Emission reduction benefit cost
C_g	Per-unit cost of microgrid
E_S	Energy served
E_{NS}	Energy not served
E_{BES}	Energy stored in battery
E_{BES}^{min}	Minimum stored energy limit of battery
E_{BES}^{max}	Maximum stored energy limit of battery
E_{SC}	Energy stored in supercapacitor
E_{SC}^{max}	Maximum stored energy limit of supercapacitor
E_{SC}^{min}	Minimum stored energy limit of supercapacitor
NDE_S	Net discounted energy served
P_L	Load power demand
P_{GT}	Microgrid total power generation
P_{Cap}	Power supplied by supercapacitor
P_{Bat}	Power supplied by battery
P_{BES}^c	Battery charging power
P_{BES}^d	Battery discharging power
P_{PV}	Power supplied by PV
P_{WT}	Power supplied by WT
P_{gap}	Difference between generation and demand
P_{gap-L}	Low frequency component of P_{gap}
P_{gap-H}	High frequency component of P_{gap}
P_G	Power generated by wind and solar
$\boldsymbol{\Delta P}$	Cumulative error matrix
P_{BES}^{cmax}	Battery charging power limit
P_{BES}^{dmax}	Battery discharging power limit
P_{BES}^c	Battery charging power
P_{BES}^d	Battery discharging power
P_{SC}^{max}	Supercapacitor power limit
P_{MG-U}	Power supplied by microgrid to utility
P_{U-MG}	Power supplied by utility to microgrid
PWF	Present worth factor
r	Uniform random number
$\mathbf{RS_{space}}$	Reduced search space
$\mathbf{S_{space}}$	Search space
$\boldsymbol{SS}$	Solution space
T_o	Atmospheric temperature
v	Wind speed
ω_o	Cut-off frequency

I. INTRODUCTION

During the past few decades, rising concerns for global warming and volatile fossil fuels prices have made renewable energy (RE) sources an attractive alternative. This trend has been further underpinned by rapid advancements in the power electronics field, which enabled full controllability of RE sources, within the constraints inflicted by the natural phenomenon [1]. The integration of RE sources in electric power grid has evolved into the concept of microgrid (MG). MGs are state-of-the-art active distribution networks consisting of distributed generators (DGs), energy storage system (ESS), and flexible loads, operated grid-connected or islanded, in a controlled, coordinated way [2]. Due to the propinquity of DGs to the loads in MGs and the utilization of RE sources, MGs are trusted to supply its customers with more efficient and eco-friendly energy, reduced power losses and network congestion, and improved power quality and reliability compared to the energy supplied by conventional power plants. MGs are contemplated to be an integral part of smart grids in the future electric power system.

Solar and wind are two expeditiously emerging RE sources, especially solar has gained more popularity due to significant decline in its cost over the past few years. Since, such sources are intermittent, uncontrollable, stochastic, and highly variable, their integration in the electric power grid poses challenges to its effective operation, especially at higher penetration levels. For example, load mismatch, poor load following, voltage instability, frequency deviation, inferior power quality, and reliability problems are some of

the detrimental impacts that RE sources introduce in electric power network [3]. New, innovative technologies and novel ideas are required to alleviate the aforementioned problems, to increase the penetration of RE sources in the electric power grid.

A potential candidate solution to the aforesaid problems is to store energy during surplus generation hours using ESS and redispatch it appropriately later when needed [4]–[8]. Several types of ESS are available and among them battery energy storage (BES) system is most frequently utilized [9]–[11]. But batteries are only efficient at supplying low steady loads, while outputs of RE sources are highly fluctuating, which are not suitable for them. It is difficult for batteries to recover from rapid power swings without a significant reduction in their lifetime [12]. An ideal ESS must have a high power density to follow rapid power fluctuations, a high energy density to give autonomy to the electric power grid, and longer life. As a sole energy storage technology is unlikely to deliver these essentials effectively and economically, it is vital to couple multifarious energy storage technologies, creating a hybrid energy storage system (HESS).

Most recently, HESS has become an emergig storage technology as it combines the benefits of multiple technologies. For example, BES and SC can be combined to build HESS. The BES systems have high specific energy, low specific power, low self-discharge, low cycle life, long charge times, and relatively lower cost per watt-hour. On the other hand, the SC storage systems have low specific energy, high specific power, high cycle life, very high self-discharge, short charge times, and high cost per watt-hour [13], [14]. The HESS makes use of complementary properties of BES and SC and provides large energy supply, high power, and fast dynamic response at the same time economically and effectively [15]–[18]. Nevertheless, to optimize the lifetime of both BES and SC, it is vital to ensure that both operate within their operational constraints. BES must operate within its state of charge and current bounds and SC within its voltage and current bounds. At the same time the SC should respond to rapid large current signals in order to maximize the lifespan of BES [19]. It is also important to note that the cost of energy storage units per kilowatt is a strong function of their capacity, and too high cost is prohibitive to commercial and industrial acceptance, a method for optimizing the size and operation of such HESS to fit application constraints is a crucial task. In this paper, BES and SC storage technologies will be combined to build up a HESS as shown in Fig. 1.

This paper proposes a methodology for the capacity optimization of a residential MG employing hybrid PV-WT and BES-SC. The proposed method benefits from multidisciplinary fields. For example, battery storage technology, SC technology, RE technology, control theory with an efficient co-ordination within the subsystems. For instance, very precise co-ordination is required for the operation of HESS specifically at the switching instance otherwise the full benefits of HESS will not be harnessed. The sizing problem is formulated and it is a complex optimization problem,

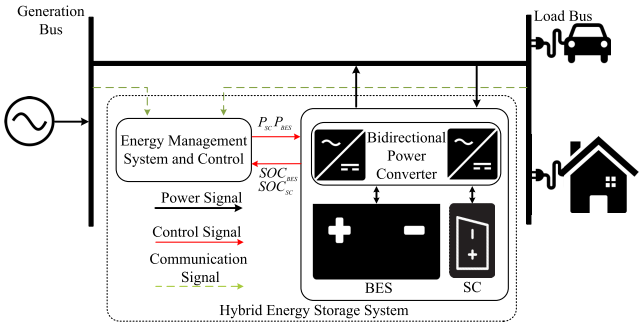

FIGURE 1. A hybrid energy storage system.

subjected to variety of realistic constraints both from hybrid generation and storage, and an objective function is proposed to (i) minimize the cost, (ii) improve the reliability, and (iii) curtail green house gases (GHG) emissions. The complex optimization problem is solved innovatively in piecewise fashion to reduce the complexity and computational time. First, combinations of optimal sizes of PV and WT are determined out of several possible combinations using an advanced constraint based innovative search algorithm, and in the second step, size of HESS is calculated for each combination. Finally, the optimal solution is determined based upon the minimum value of the cost function. The main contributions of our work is that we propose a technique for combined capacity optimization of hybrid generation, i.e., WT-PV system and the HESS comprising of BES and SC employed in grid-connected MG. As, instead of a single energy storage or renewable energy source, we consider hybrid power generation with hybrid energy storage, and optimize their capacities. This optimization exploits the benefits from each individual element, and therefore the solution achieved is more cost efficient, highly reliable and eco-friendlier.

As a case study, the proposed methodology is validated using real-world data of wind speed, solar irradiation and power demand from Dammam city in Saudi Arabia.

The remainder of the paper is organized as follows. Section II presents the related work and detailed MG modeling is discussed in Section III. The proposed methodology is demonstrated in Section IV. The information of the databases is provided in Section V. The Section VI presents results and discussions and conclusion is given in Section VII.

II. RELATED WORK

Different methods have been proposed in literature for sizing of MG and we will briefly review some of them here. In [20], sizing of PV, WT, and ESS is done based on minimization of total planning cost. In [21], genetic algorithm is used to determine the optimal sizes of PV, WT, diesel, and BES based upon cost, carbon emissions, and dump energy. In [22], sizing of WT, PV, BES, and fuel cell is done based on the cost and reliability. In [23], optimal sizes of PV, WT, diesel generator, BES, and pumped storage are determined based upon minimizing both initial investment and operational/maintenance

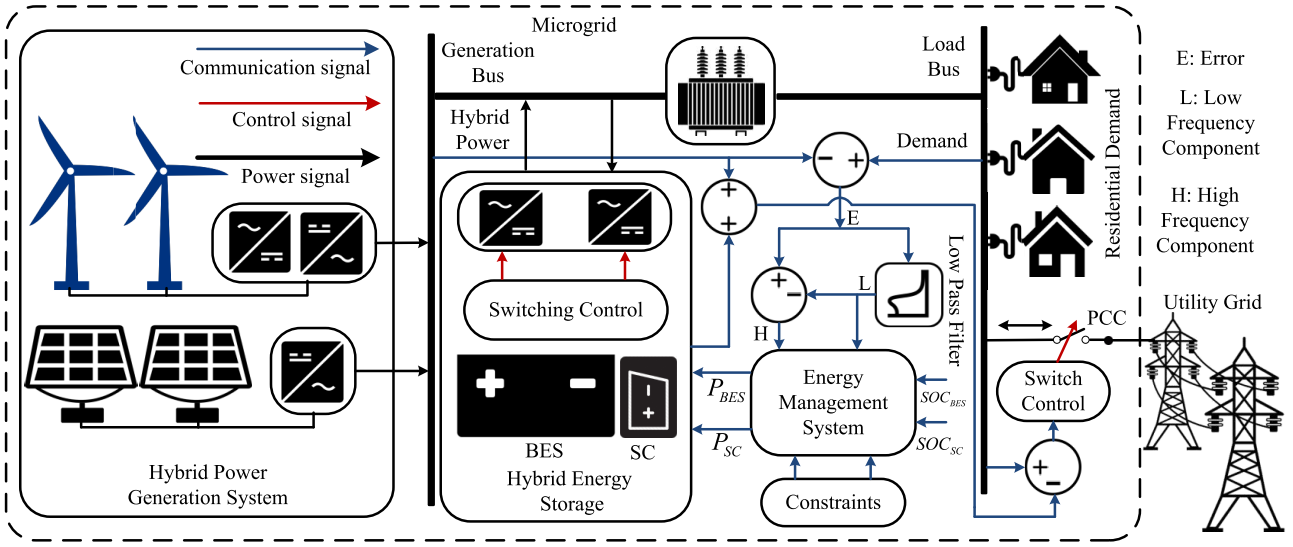

FIGURE 2. Block diagram of grid-connected MG system.

costs. In [24], sizes of PV, WT, and BES are determined using mixed integer linear programming. In [25], capacity optimization of PV, WT, diesel generator, BES, fuel cell, electrolyzer, and hydrogen tank is done based upon cost minimization, GHG emissions, and reliability using particle swarm optimization (PSO). In [26], optimal sizes of PV, WT, and BES are determined considering multiple objectives, i.e., cost minimization, and higher supply reliability. In [27], optimal sizing of MG comprising of WT, PV, BES, and biomass is done considering two alternative objectives, i.e., minimization of total annual energy losses and cost of energy. In [28], optimal sizing and sitting of renewable DGs is done based upon the minimization of annual investment cost and operation cost. In [29], planning of PV, WT, and BES grid-connected MG is done based upon cost minimization and customer satisfaction maximization, and mixed integer linear programming is used to solve the optimization problem. In [30], optimal sizing of PV, WT, and BES based residential MG is done considering the cost minimization objective. In [31], capacity optimization of PV and BES is done based upon levelized cost of energy. In [32], capacity optimization of PV, WT, tidal turbine, and BES is done based upon the net present cost and reliability, the optimization problem is solved using crow search algorithm. In [33], optimal sizes of PV, WT, diesel generator, biodiesel generator, fuel cell, and BES are determined based on minimization of cost of energy. In [34], optimization of BES-SC is done based upon initial investment cost and simulated annealing PSO is used to solve the optimiztion problem. In [35], a statistical approach is used to optimize the size of the BES-SC hybrid storage system.

It is important to understand that the size of ESS depends upon the behavior of load, wind power, and solar power. So, optimal size of ESS determined for a particular geographical location cannot be considered as optimal for any other location even with same installed capacities of RE sources. Thus, to harvest maximum benefits it is necessary to optimize RE sources and ESS altogether. Also, BES systems have limited number of cycles. One of the primary purposes of hybridization of BES system with SC storage technology is to prolong the lifespan of BES system. Therefore, it is also vital to consider the cycles of BES system while optimizing BES-SC system. Moreover, initial investment cost, operation and maintenance cost, replacement cost, reliability, and GHG emissions should be considered in the objective function to get more optimized results. It is clearly evident from the existing literature, the researchers have considered these aforementioned parameters in their formulations, however, considering sum of parameters is important but in most of the cases, formulations are based upon one parameter only. For example, [34] has optimized the size of BES-SC energy storage based upon initial investment cost.

In general, the literature deals with the capacity optimization of MGs employing single or multiple RE sources, conventional DGs, ESS, and variety of loads, operating in grid-connected or islanded mode based upon cost or cost-reliability. And to date, to the best knowledge of authors no methodology has been developed for the joint capacity optimization of the emerging hybrid PV-WT and ultramodern BES-SC system employed by a grid-connected MG system.

III. MICROGRID MODELLING

The block diagram of the MG considered in this study is shown in Fig. 2, it utilizes PV-WT for hybrid power generation and BES-SC for hybrid energy storage. A hybrid RE system, employing two or more RE sources, mitigates the intermittent nature of RE resources to some extent and also improves the system efficiency [21]. The PV and WT are coupled to generation bus through DC/AC and AC/AC converters respectively, and HESS is connected to AC bus via

bidirectional DC/AC converter. The residential load is taped from the load bus via step down coupling transformers, and the utility grid (UG) is also connected to the load bus at point of common coupling (PCC) through a controlled switch.

A. WIND POWER GENERATION SYSTEM

A WT generates electrical energy from kinetic energy of wind. Weibull distribution function can be used to estimate the wind speed as

$$F(v) = 1 - exp\left(-\left(\frac{v}{c}\right)^{\sigma}\right) \quad (1)$$

$$v = c\left[-ln(1-r)\right]^{\frac{1}{\sigma}} \quad (2)$$

$$v = c\left[-ln(r)\right]^{\frac{1}{\sigma}} \quad (3)$$

where σ is shape factor, c is scale factor, v is wind speed in m/sec and, r is uniform random number. The values of σ and c of any geographical location can be obtained from the historical data. Using the wind speed the power output of a WT can be calculated as [36].

$$P_{WT}(v) = \begin{cases} 0 & v < v_{ci} \\ P_{rated} \times \dfrac{v - v_{ci}}{v_r - v_{ci}} & v_{ci} \le v < v_r \\ P_{rated} & v_r \le v < v_{co} \\ 0 & v \ge v_{co} \end{cases} \quad (4)$$

where v_{ci}, v_r, and v_{co} are cut-in, rated, and cut-out speeds respectively, P_{WT} is the output power of WT, and P_{rated} is the rated power of WT. From (4) the power output of WT is zero below v_{ci} and above v_{co}, and the output power increases linearly with the increase in the wind speed between v_{ci} and v_r, and it generates rated power between v_r and v_{co}.

B. SOLAR PHOTOVOLTAIC GENERATION SYSTEM

A solar PV generation system converts solar energy to electrical energy. The output power of a PV system depends upon solar irradiation, atmospheric temperature, area and efficiency of the PV array. It is assumed that a maximum power point tracker is installed to extract the maximum of available power. The hourly output power of a PV system is calculated as

$$P_{PV}(t) = \eta_{PV} A I(t)\left(1 - 0.005\left(T_o(t) - 25\right)\right) \quad (5)$$

where η_{PV} is the efficiency and A is the area in m^2 of the solar cell array, I is the solar irradiation in kW/m^2, and T_o is the atmospheric temperature in ^oC.

C. BATTERY ENERGY STORAGE SYSTEM

A BES system consists of series and parallel strings of batteries. In this work, a sodium sulphur (NaS) battery is considered. NaS is one of the batteries used for commercial electrical energy storage in electric utility distribution grid support, wind power integration, and high-value grid services. Its applications include load levelling, peak shaving, and power quality as well as renewable energy management and integration. A BES model, as given in [37], is calculated as

$$Charge: E_{BES}(t + \Delta t) = E_{BES}(t) + \Delta t P^c_{BES} \eta_c \quad (6)$$

$$Disharge: E_{BES}(t + \Delta t) = E_{BES}(t) - \Delta t \frac{P^d_{BES}}{\eta_d} \quad (7)$$

Charging/discharging constraints are

$$0 \le P^c_{BES} \le P^{cmax}_{BES} \quad (8)$$

$$0 \le P^d_{BES} \le P^{dmax}_{BES} \quad (9)$$

Stored energy bounds are

$$E^{min}_{BES} \le E_{BES}(t) \le E^{max}_{BES} \quad (10)$$

where E_{BES} is the energy stored in the battery, i.e., state-of-charge, P^c_{BES} and P^d_{BES} are charging and discharging powers respectively, and η_c is charging efficiency and η_d is discharging efficiency of the battery.

D. SUPERCAPACITOR

Energy stored in the SC at any instant is modeled as

$$E_{SC}(t + \Delta t) = E_{SC}(t) + \eta \Delta t P_{SC} - \xi E_{SC}(t) \quad (11)$$

subjected to the following constraints

$$E^{min}_{SC} \le E_{SC}(t) \le E^{max}_{SC} \quad (12)$$

$$0 \le P_{SC}(t) \le P^{max}_{SC} \quad (13)$$

where E_{SC} is the energy stored in SC, η is charging/discharging efficiency, ξ is self-discharge rate, and P_{SC} is the power supplied/drawn to/from the SC. During charging period P_{SC} is positive while it is negative during discharging period. The (12) represents the stored energy constraint whereas (13) represents the bounds for power supplied/drawn to/from the SC.

E. UTILITY GRID

Utility grid serves two important objectives, (i) ensures load and generation always to be equal by supplying the demand whenever MG generation is lower than demand, and (ii) buys energy from the MG during surplus generation hours to make the system more economical. The power of UG at any instant of time can be modeled as

$$P_{grid}(t) = P_L(t) - \sum\left(P_{WT}(t), P_{PV}(t), P_{BES}(t), P_{SC}(t)\right) \quad (14)$$

where P_{grid} is the power supplied to/from the UG, P_L is load demand, P_{BES} is the power supplied by BES and P_{SC} is the power supplied by SC. During surplus generation hours P_{grid} is negative while positive during inadequate supply hours.

IV. PROPOSED METHODOLOGY

The proposed methodology is further divided into five subsections. Section IV-A presents methodology for sizing of RE sources, and HESS sizing strategy is discussed in detail

in Section IV-B. Reliability and economic modeling is discussed in Section IV-C, while modeling of GHG emissions is presented in Section IV-D. Finally, the objective function formulation is given in Section IV-E.

A. RENEWABLE ENERGY SOURCES SIZING

Consider a hybrid PV-WT generation system as shown in Fig. 2. Power generated by the system is calculated as follows

$$P_G^{(i,j)}(t) = N_{PV}^i P_{PV}(t)\, PV_{status}^i(t) + N_{WT}^j P_{WT}(t)\, WT_{status}^j(t) \quad \forall i \in [1, i_{max}], j \in [1, j_{max}], t > 0 \tag{15}$$

where

$$PV_{status}^i(t) = \begin{cases} 0 & G_{PV}^i(t) < FOR_{PV} \\ 1 & otherwise \end{cases} \quad \forall i, t > 0$$
$$G_{PV}^i(t) = rand\ () \tag{16}$$

and

$$WT_{status}^j(t) = \begin{cases} 0 & G_{WT}^j(t) < FOR_{WT} \\ 1 & otherwise \end{cases} \quad \forall i, t > 0$$
$$G_{WT}^j(t) = rand\ () \tag{17}$$

subjected to the following constraints

$$N_{PV}^{min} \le N_{PV}^i \le N_{PV}^{max}$$
$$N_{WT}^{min} \le N_{WT}^j \le N_{WT}^{max}$$

where P_G is the renewable generated power, N_{PV} and N_{WT} are the number of PVs and WTs, P_{PV} and P_{WT} are the powers generated by single PV and WT, and PV_{status} and WT_{status} are the statuses of PVs and WTs which decide whether they would generate power or not. When the value of PV_{status} of a solar PV is 0 that means the solar PV cannot generate power because of some fault or any other reason. As given in (16) and (17), values of PV_{status} and WT_{status} are calculated using forced outage rates FOR_{PV} and FOR_{WT}. G_{PV} and G_{WT} are random numbers which are generated using the rand () command of MATLAB. N_{PV}^{min}, N_{WT}^{min}, N_{PV}^{max}, and N_{WT}^{max} are minimum and maximum number of PVs and WTs which are calculated using following relations:

$$N_{PV}^{min} = \frac{\sum_{t=1}^{n} \alpha P_L(t)}{\sum_{t=1}^{n} P_{PV}(t)} \tag{18}$$

$$N_{WT}^{min} = \frac{\sum_{t=1}^{n} \beta P_L(t)}{\sum_{t=1}^{n} P_{WT}(t)} \tag{19}$$

$$N_{PV}^{max} = \frac{\sum_{t=1}^{n} \gamma P_L(t)}{\sum_{t=1}^{n} P_{PV}(t)} \tag{20}$$

$$N_{WT}^{max} = \frac{\sum_{t=1}^{n} \rho P_L(t)}{\sum_{t=1}^{n} P_{WT}(t)} \tag{21}$$

where α, β, γ, and ρ are scaling factors and n is the total number of intervals. The instantaneous error between load and generation is calculated as follows

$$\Delta p^{(i,j)}(t) = P_L(t) - P_G^{(i,j)}(t) \quad \forall i, j, t > 0 \tag{22}$$

where Δp is the instantaneous error. Cumulative error ΔP is the sum of absolute values of all instantaneous errors.

$$\Delta P^{(i,j)}(t) = \sum_{t=1}^{n} \left(|\Delta p^{(i,j)}(t)| \right) \quad \forall i, j, t > 0 \tag{23}$$

where $\Delta P^{(i,j)}$ is the cumulative error corresponding to N_{PV}^i and N_{WT}^j. A smaller value of the cumulative error means that intermittent generation follows load demand effectively. While a larger value of the cumulative error shows that there is a significant difference between load and generation. All cumulative errors are stored in a matrix as

$$\boldsymbol{\Delta P} = \begin{bmatrix} \Delta P^{(1,1)} & \cdots & \Delta P^{(1,j_{max})} \\ \vdots & \ddots & \vdots \\ \Delta P^{(i_{max},1)} & \cdots & \Delta P^{(i_{max},j_{max})} \end{bmatrix}_{(i_{max} \times j_{max})} \tag{24}$$

where $\boldsymbol{\Delta P}$ is the matrix that contains the values of the cumulative errors for every possible combination of N_{PV} and N_{WT}. The values of N_{PV} and N_{WT} that correspond to each ΔP are stored in the vectors $\boldsymbol{N_{PV}}$ and $\boldsymbol{N_{WT}}$ as follows

$$\mathbf{N_{PV}} = \begin{bmatrix} N_{PV}^{min} & \cdots & N_{PV}^{max} \end{bmatrix}^T \tag{25}$$
$$\mathbf{N_{WT}} = \begin{bmatrix} N_{WT}^{min} & \cdots & N_{WT}^{max} \end{bmatrix} \tag{26}$$

A search space has been formulated by using (24)-(26) as

$$\mathbf{S_{space}} = \begin{bmatrix} 0 & \mathbf{N_{WT}} \\ \mathbf{N_{PV}} & \boldsymbol{\Delta P} \end{bmatrix}_{(i_{max}+1) \times (j_{max}+1)} \tag{27}$$

where $\mathbf{S_{space}}$ is the search space which contains all possible combinations of N_{PV} and N_{WT} and their corresponding cumulative errors. The $\mathbf{S_{space}}$ is reduced by selecting the minimum value of the ΔP from its each column as follows

$$\boldsymbol{\Delta P_{min}} = \begin{bmatrix} \Delta P_{min}^1 & \cdots & \Delta P_{min}^{j_{max}} \end{bmatrix}_{1 \times j_{max}} \tag{28}$$

where

$$\Delta P_{min}^j = min\left(\mathbf{S_{space}}(z, j)\right) \quad \forall j$$
$$z = 2, ..., i_{max} + 1 \tag{29}$$

where $\boldsymbol{\Delta P_{min}}$ is the vector which contains the minimum values of cumulative errors, i.e., ΔP_{min} extracted from the $\mathbf{S_{space}}$. The values of N_{PV} and N_{WT} that correspond to the minimum values of the cumulative errors are stored in the following vectors as

$$\mathbf{N_{PV_{min}}} = \begin{bmatrix} N_{PV_{min}}^1 & \cdots & N_{PV_{min}}^{j_{max}} \end{bmatrix}_{j_{max} \times 1}^T \tag{30}$$
$$\mathbf{N_{WT_{min}}} = \begin{bmatrix} N_{WT_{min}}^1 & \cdots & N_{WT_{min}}^{j_{max}} \end{bmatrix}_{1 \times j_{max}} \tag{31}$$

A reduced search space is formulated using (28)-(31) as

$$\mathbf{RS_{space}} = \begin{bmatrix} \boldsymbol{\Delta P_{min}}^T & \mathbf{N_{PV_{min}}} & \mathbf{N_{WT_{min}}}^T \end{bmatrix}_{j_{max} \times 3} \tag{32}$$

where $\mathbf{RS_{space}}$ is the reduced search space. There are j_{max} combinations of $N_{PV_{min}}$ and $N_{WT_{min}}$ in $\mathbf{RS_{space}}$ for which there will be j_{max} optimal storage sizes, one for each combination.

B. HYBRID ENERGY STORAGE SYSTEM SIZING

Power generated by any combination selected from the reduced search space is calculated using following equation

$$P_G^u(t) = N_{PV}^{min^u} P_{PV}(t) + N_{WT}^{min^u} P_{WT}(t) \quad \forall t > 0 \tag{33}$$

subjected to following constraints

$$N_{PV}^{min^1} \leq N_{PV}^{min^u} \leq N_{PV}^{min^j_{max}}$$
$$N_{WT}^{min^1} \leq N_{WT}^{min^u} \leq N_{WT}^{min^j_{max}}$$

where P_G is the power generated by the MG and u is the case number. The difference between power generated and power demanded for case u at any instant of time is denoted by p_{gap}^u and calculated as follows

$$p_{gap}^u(t) = P_L(t) - P_G^u(t) \quad \forall t > 0 \tag{34}$$

The p_{gap} is divided into two components, i.e., high frequency and low frequency components as shown in Fig. 2. The high frequency component is used for the sizing of SC and the low frequency component is used for the sizing of BES. The algorithm for dividing p_{gap} into high and low frequency components can be realized by low pass energy filter whose transfer function is given below

$$H(s) = \frac{K\omega_o^2}{s^2 + (\omega_o/Q) + \omega_o^2} \tag{35}$$
$$p_{gap}^u = p_{gap-H}^u + p_{gap-L}^u \tag{36}$$

where ω_o is cut-off frequency, p_{gap-H} is high frequency component, and p_{gap-L} is low frequency component. The maximum capacities of BES and SC that can be employed to store all of the excess energy are determined by using the algorithms given below. These algorithms represent the operation of BES and SC based upon which their maximum capacities, that can be installed, have been calculated.

$$P_{gap-H}^u(\hbar) = \begin{cases} P_{gap-H}^u(\hbar) & P_{gap-H}^u(\hbar) > 0 \\ 0 & otherwise \end{cases} \quad \forall \hbar \tag{37}$$

where

$$P_{gap-H}^u(\hbar) = \sum_{t=1}^{\hbar} p_{gap-H}^u(t) \tag{38}$$

The maximum SC size is calculated as

$$C_{max}^u = max(P_{gap-H}^u) \tag{39}$$

Similarly, for BES we have

$$P_{gap-L}^u(\hbar) = \begin{cases} P_{gap-L}^u(\hbar) & P_{gap-L}^u(\hbar) > 0 \\ 0 & otherwise \end{cases} \quad \forall \hbar \tag{40}$$

where

$$P_{gap-L}^u(\hbar) = \sum_{t=1}^{\hbar} p_{gap-L}^u(t) \tag{41}$$

The maximum capacity of BES is calculated as

$$B_{max}^u = max(P_{gap-L}^u) \tag{42}$$

where B_{max} and C_{max} are the maximum capacities of BES and SC. Required capacities of BES and SC would be less than or equal to B_{max} and C_{max} which are calculated as

$$B_{cap}^u = \begin{cases} B_{max}^u & x = 1 \\ CBS^u & x = 0 \end{cases} \tag{43}$$

where B_{cap} is the required energy capacity of battery. The B_{cap} is equal to B_{max} if the battery discharges completely after the full charging period and this condition is indicated by $x = 1$. While the B_{cap} is equal to corrected battery size CBS if the battery does not discharge fully after its full charging period, this condition is indicated by $x = 0$. The condition $x = 0$ implies that the battery is over-sized. An iterative region elimination algorithm is used to calculate CBS which is defined by following equations:

$$CBS^u(w) = \frac{S_{min}^u(w) + S_{max}^u(w)}{2} \tag{44}$$

where

$$S_{min}^u(w+1) = \begin{cases} S_{min}^u(w) & x = 1 \\ CBS(w) & x = 0 \end{cases} \tag{45}$$

and

$$S_{max}^u(w+1) = \begin{cases} S_{max}^u(w) & x = 0 \\ CBS(w) & x = 1 \end{cases} \tag{46}$$
$$STEP_a^u = S_{max}^u(w) - S_{min}^u(w) \tag{47}$$

where S_{min} and S_{max} are the minimum and maximum boundaries of solution, $STEP_a$ is the difference between the minimum and maximum boundaries, and w is the iteration number. Initially, S_{min} and S_{max} are set equal to 0 and B_{max} respectively. Both of them get updated in an iterative fashion until $STEP_a$ becomes less than or equal to the allowable tolerance e. Similar calculations that are given in (43)-(47) can be repeated (just with a little modification in the constraints while calculating x) to find the required size of SC (C_{cap}). The B_{cap} and C_{cap} are the required sizes but both are not optimal. If they are installed, the system will be reliable but not efficient and economical.

An important parameter that needs to be checked is utilization factor; higher value of utilization factor reduces the idle time and ensures the maximum benefit from BES and SC. Therefore, utilization factor is used to determine the optimal capacities of BES and SC. In order to calculate the utilization factor, battery decision variable BDV is computed as

$$BDV^u = \frac{\sum B_{chg-dcg}^u(t)}{n} \quad \forall t > 0 \tag{48}$$

where

$$B_{chg-dcg}^u(t) = \begin{cases} 1 & |P_{gap}^u(t) - P_{gap}^u(t-\Delta t)| \geq \lambda P_{BES_{max}}^u \\ 0 & else \end{cases} \quad \forall t > 0 \tag{49}$$

where $B_{chg-dcg}$ is the battery charging and discharging factor which is equal to one when the charging or discharging power

is greater than or equal to $\lambda P_{BES_{max}}$, where λ is a constant which can take a value btween 0 and 1. Hence, optimal size of BES is calculated as

$$B^u_{opt} = \begin{cases} B^u_{cap} & BDV^u \geq B_{lim} \\ BCS^u & else \end{cases} \quad (50)$$

where B_{opt} is the optimal capacity of BES and B_{lim} is the minimum battery utilization limit. The B_{opt} equals to B_{cap} if BDV becomes greater than or equal to B_{lim} otherwise B_{opt} equals to battery corrected size BCS. The BCS is calculated using a region elimination iterative search algorithm as following

$$BCS^u(w) = \frac{OCF^u_{min}(w) + OCF^u_{max}(w)}{2} \quad (51)$$

where

$$OCF^u_{min}(w+1) = \begin{cases} OCF^u_{min}(w) & BDV^u \geq BU_{lim} \\ BCS^u(w) & else \end{cases} \quad (52)$$

and

$$OCF^u_{max}(w+1) = \begin{cases} BCS(w) & BDV^u \geq BU_{lim} \\ OCF^u_{max}(w) & else \end{cases} \quad (53)$$

$$STEP^u_b = OCF^u_{max}(w) - OCF^u_{min}(w) \quad (54)$$

where OCF_{min} and OCF_{max} are the minimum and maximum boundaries of solution respectively and $STEP_b$ is the error between minimum and maximum boundaries. Initially, OCF_{min} and OCF_{max} are set equal to 0 and B^u_{cap} and both of them get updated in the iterative algorithm until $STEP_b$ reaches below the allowable tolerance e. Similar calculations that are given in (50)-(54) are repeated (just with a little modification in the constraints while calculating BDV) to find optimal size of SC (C_{opt}). A suitable value of ω_o for every combination of $\mathbf{RS_{space}}$ is determined using particle swarm optimization (PSO) technique to calculate the B_{opt} and C_{opt}.

C. RELIABILITY AND ECONOMIC MODELING

Reliability and cost are two important parameters that can be used to analyze the performance of a system. A power system having lower cost, higher reliability (i.e., energy served), and lower GHG emissions can be considered to have better performance. In this study, the optimal solution is determined on the basis of cost, reliability, and GHG emissions.

The total generation of MG after finding the optimal size of the HESS, i.e., B_{opt} and C_{opt} for u^{th} combination of PV and WT is calculated as following

$$P^u_{GT}(t) = N^{min^u}_{PV} P_{PV}(t) + N^{min^u}_{WT} P_{WT}(t) + P^u_{Bat}(t) + P^u_{Cap}(t) \quad (55)$$

where P_{GT} is the total power generated by MG, P_{Bat} is the power supplied by battery and P_{Cap} is the power supplied by SC. Energy served is the summation of demand that is served by the MG over a period of its operation.

$$E^u_S = \sum_{t=1}^{n} D^u(t) \quad (56)$$

where

$$D^u(t) = \begin{cases} P_L(t) & P^u_{GT}(t) \geq P_L(t) \\ P^u_{GT}(t) & otherwise \end{cases} \quad \forall t > 0 \quad (57)$$

where E_S is energy served, P_L is the load power demand, and P_{GT} is total generation of the MG. Energy not served E_{NS} is the summation of demand that is not supplied by the MG during its operation.

$$E^u_{NS} = \sum_{t=1}^{n} G^u(t) \quad (58)$$

where

$$G^u(t) = \begin{cases} P_L(t) - P^u_{GT}(t) & P_L(t) > P^u_{GT}(t) \\ 0 & otherwise \end{cases} \quad \forall t > 0 \quad (59)$$

Net discounted energy served is calculated as

$$NDE^u_S = E^u_S PWF \quad (60)$$

where

$$PWF = \left[\frac{(1+d)^l - 1}{d\,(1+d)^l} \right] \quad (61)$$

where PWF is the present worth factor, l is the year of operation, and NDE^u_S is the net discounted energy served by the MG.

As discussed earlier, cost is also an important parameter that can be used to assess the performance of a system. In this work initial investment cost, fixed and variable operation and maintenance costs, storage replacement cost, and cost of energy exchanged between MG and UG are considered. The following relation is used to determine the investment cost associated with RE sources

$$C^u_{inv-sc} = \sum_{k=1}^{N} C^k_{c,sr} P^{k,u}_{sr} \quad (62)$$

where C_{inv-sc} is the total investment cost of RE sources, $C^k_{c,sr}$ is the capital cost of k^{th} source in \$/MW, P^k_{sr} is the installed capacity of k^{th} source in MW, and N is the total number of RE sources. The investment cost of storage system is calculated as follows

$$C^u_{inv-stg} = \sum_{k=1}^{M} \left(C^k_{c,stg} E^{k,u}_{stg} + C^k_{c,pcs} P^{k,u}_{stg} \right) \quad (63)$$

where $C^k_{c,stg}$ is the capital cost of k^{th} storage unit in \$/MWh, E^k_{stg} is the energy capacity of k^{th} storage unit in MWh, $C^k_{c,pcs}$ is the cost of power conditioning system required for the storage in \$/MW, P^k_{stg} is the power capacity of k^{th} storage unit in MW, and M is the total number of storage units. The replacement cost of storage is modeled as following

$$C^{k,u}_{rep-stg} = \sum \frac{C^k_{c,stg} E^{k,u}_{stg}}{(1+d)^s} \quad s = p, 2p, 3p, ...l - p \quad (64)$$

where d is the discount rate and p is the life of the storage in years. The operation and maintenance costs of the MG

consist of fixed and variable operation and maintenance costs are calculated as follows

$$C^u_{om} = C^u_{om,f} + C^u_{om,v} \tag{65}$$

where

$$C^u_{om,f} = \sum_{t=1}^{n} \sum_{k=1}^{M+N} T^k(t) J^k_{om,f} P^k_r \tag{66}$$

and

$$C^u_{om,v} = \sum_{t=1}^{n} \sum_{k=1}^{M+N} J^k_{om,v} P^k(t) \tag{67}$$

where $C_{om,f}$ is the fixed operation and maintenance cost, T^k is the time of operation of k^{th} element, $J^k_{om,f}$ is the operation and maintenance cost factor in \$/MW-yr, and P^k_r is the rated power capacity of k^{th} element in MW. The variable operation and maintenance cost is referred by $C_{om,v}$, $J^k_{om,v}$ is the variable operation and maintenance cost factor in \$/MW, and $P^k(t)$ is the output power of k^{th} element at time t in MW. Net present value of C_{om} is calculated as

$$NPVC^u_{om} = C^u_{om} PWF \tag{68}$$

where $NPVC_{om}$ is the present worth of C_{om}.

During surplus generation hours, the MG sells energy to UG. Total cost and net present worth of the energy supplied by MG to UG is calculated as follows

$$C^u_{MG-U} = \sum_{t=1}^{n} C_{exchg}(t) P^u_{MG-U}(t) \tag{69}$$

$$NPVC^u_{MG-U} = C^u_{MG-U} PWF \tag{70}$$

where C_{MG-U} is the total cost of the energy sold by MG to UG, $C_{exchg}(t)$ is the cost at time t, $P_{MG-U}(t)$ is the power supplied by MG to UG at time t, and $NPVC_{MG-U}$ is the present worth of C_{MG-U}. In the event when MG generation is insufficient to meet the demand, the MG buys power from UG. Total cost and net present worth of energy supplied by the utility to MG is calculated using following equations

$$C^u_{U-MG} = \sum_{t=1}^{n} C_{exchg}(t) P^u_{U-MG}(t) \tag{71}$$

$$NPVC^u_{U-MG} = C^u_{U-MG} PWF \tag{72}$$

where C_{U-MG} is the total cost of energy supplied by UG to MG, $C_{exchg}(t)$ is the cost at time t, $P_{U-MG}(t)$ is the power supplied by UG to MG at time t, and $NPVC_{U-MG}$ is the present worth of C_{U-MG}.

D. MODELING OF GHG EMISSIONS

When electric power is generated by burning fossil fuels, it results in GHG emissions in the environment. There is a correction cost which is needed to mitigate the damage caused by these emissions as shown in Table 1. This correction cost would be a saving if the electric power is generated by utilizing RE sources instead of fossil fuels. This saving is named as emission reduction benefit cost (ERBC), and modeled as

TABLE 1. Greenhouse gases emission data.

Greenhouse gases	CO_2	CO	SO_2	NOx
Emissions kg/MWh	1000.7	1.55	9.993	6.46
Correction Cost \$/kg	0.0037	0.16	0.97	1.29

$$C^u_{ERB} = \sum_{k=1}^{4} \sum_{t=1}^{n} P^u_{GT}(t) E^k E^k_{cc} \tag{73}$$

where C_{ERB} is the total ERBC, $P_{GT}(t)$ is the power output of MG at time t, E^k is the emission of k^{th} type of GHG, and E^k_{cc} is the cost required to correct the damage caused by k^{th} type of GHG. The net present value of total ERBC is calculated using following equation as

$$NPVC^u_{ERB} = C^u_{ERB} PWF \tag{74}$$

where $NPVC_{ERB}$ is the present worth of ERBC.

E. COST FUNCTION FORMULATION

The objective is to find an optimal combination of PV, WT, BES, and SC that must result in lower cost, higher reliability, and lower GHG emissions. Cost function of the optimization problem is formulated as following

$$obj: F^u = \sqrt{\left(f^u_1(\boldsymbol{X_1}^u, \boldsymbol{X_2}^u) - f^u_2(\boldsymbol{X_1}^u, \boldsymbol{X_2}^u)\right)^2} \rightarrow \min \tag{75}$$

$$s.t. \begin{cases} \boldsymbol{g}_\ell(\boldsymbol{X_1}^u, \boldsymbol{X_2}^u) = 0 & \ell = 1, 2, , \ldots, m \\ \boldsymbol{h}_\iota(\boldsymbol{X_1}^u, \boldsymbol{X_2}^u) \leq 0 & \iota = 1, 2, , \ldots, q \end{cases} \tag{76}$$

where

$$\boldsymbol{X_1}^u = \left[N^{min^u}_{PV},\ N^{min^u}_{WT},\ P^u_{Cap},\ P^u_{Bat}\right] \tag{77}$$

and

$$\boldsymbol{X_2}^u = \left[E^u_{Cap},\ E^u_{Bat},\ \omega^u_o\right] \tag{78}$$

The first term in the objective function is cost per unit of the MG. It is important to note that the initial investment cost of sources (62), initial investment cost of storage (63), operation and maintenance cost (68), replacement cost (64), cost of energy supplied by UG to MG (71), and energy served (60) are incorporated in the cost per unit of MG. Second term of the objective function represents the GHG emissions that are translated in terms of cost using ERBC concept as discussed in Section IV-D. The equality constraints are referred by $\boldsymbol{g}$ and in-equality constraints are referred by $\boldsymbol{h}$. All system constarints are summarized as:

The Pimary System Constraint (Generation = Demand):

$$P^u_{GT} + P^u_{U-MG} - P_L - P^u_{MG-U} = 0 \tag{79}$$

The hybrid power generation constraints:

$$N^{min^1}_{PV} \leq N^{min^u}_{PV} \leq N^{min^j}_{PV} \tag{80}$$

$$N^{min^1}_{WT} \leq N^{min^u}_{WT} \leq N^{min^j}_{WT} \tag{81}$$

TABLE 2. Monthly shape and scale factors.

Month	σ	c
Jan	2.40	4.77
Feb	2.45	4.85
Mar	2.55	5.15
Apr	2.40	5.06
May	2.40	5.52
Jun	2.60	6.51
Jul	2.50	5.54
Aug	2.30	4.91
Sep	2.20	4.18
Oct	2.05	4.09
Nov	2.20	4.38
Dec	2.00	4.68

BES Constraints:

$$0 \leq P_{BES}^{c} \leq P_{BES}^{cmax} \tag{82}$$

$$0 \leq P_{BES}^{d} \leq P_{BES}^{dmax} \tag{83}$$

$$E_{BES}^{min} \leq E_{BES}(t) \leq E_{BES}^{max} \tag{84}$$

SC Constraints:

$$E_{SC}^{min} \leq E_{SC}(t) \leq E_{SC}^{max} \tag{85}$$

$$0 \leq P_{SC}(t) \leq P_{SC}^{max} \tag{86}$$

Switching Frequency Constraint:

$$0 \leq \omega_o^u \leq 1 \tag{87}$$

A solution space is generated which contains the values of cost function that correspond to all j_{max} combinations of PV, WT, BES, and SC. Solution space is given as follows

$$\boldsymbol{SS} = \left[F^1\ F^2 \ldots\ F^{j_{max}}\right]_{1\times j_{max}} \tag{88}$$

where $\boldsymbol{SS}$ is the solution space and F is value of the objective function. There are j_{max} possible solutions each corresponding to one combination. The best solution from the $\boldsymbol{SS}$ is selected based upon minimum value of the cost function by using a minima search algorithm. The pseudocode of the optimal sizing is given in Algorithm I.

V. DATABASES

As mentioned earlier, the proposed methodology is tested using real-world data of wind speed, solar irradiation and power demand from Dammam city in Saudi Arabia. The Dammam city lies in the eastern province of Kingdom of Saudi Arabia and its coordinates are 26.3927N, 49.9777E. The wind speed is calculated using the shape and scale parameters of Weibull distribution. The shape and scale parameters were determined using well maintained meteorological data of wind of 20 years [38]. Monthly shape and scale parameters are given in Table 2. The normalized daily average residential power demand of the calendar year 2015 is presented in Fig. 3, which depicts that the daily peak occurs around 8 pm while minimum demand appears around 7 am. The normalized daily average solar irradiation is shown in Fig. 4 showing irradiation peak at around 1pm. Whereas the normalized daily average wind speed is shown in Fig. 5. It can be observed that wind speed is variable and fluctuates throughout the day. The economic and technical data is given in Table 3.

Algorithm 1 Optimal Capacity Sizing

Start
Initialization: $i \leftarrow 1, j \leftarrow 1, t \leftarrow 1, u \leftarrow 1, e \leftarrow 0.1$
- **Data Generation**

Read: $c, \sigma, I, \alpha, \beta, \gamma, \rho, Load$
Calculate: $P_{PV}, P_{WT}, P_L, N_{PV}^{min}, N_{WT}^{min}, N_{PV}^{max}, N_{WT}^{max}, P_G$
Save: $P_{PV}, P_{WT}, P_L, N_{PV}^{min}, N_{WT}^{min}, N_{PV}^{max}, N_{WT}^{max}, P_G$
- **Search Space Formation**

While $i \leq i_{max}$ **Do**
  While $j \leq j_{max}$ **Do**
    Calculate: $\Delta P^{(i,j)}$, $\boldsymbol{\Delta P}$
    Save: $\boldsymbol{\Delta P}$, $\mathbf{N_{PV}}$, $\mathbf{N_{WT}}$
    Calculate: $\mathbf{S_{space}}$
    $j \leftarrow j + 1$
  End While
  $i \leftarrow i + 1$
End While
- **Reduced Search Space Formation**

While $j \leq j_{max} + 1$ **Do**
  While $i \leq i_{max} + 1$ **Do**
    Calculate: $\Delta P^{j}_{min}, N^{j}_{PV_{min}}, N^{j}_{WT_{min}}$
    $i \leftarrow i + 1$
  End While
  Calculate: $\boldsymbol{\Delta P}_{\mathbf{min}}, \mathbf{N_{PV_{min}}}, \mathbf{N_{WT_{min}}}$
  $j \leftarrow j + 1$
End While
Calculate: $\mathbf{RS_{space}}$
- **HESS Sizing**

While $u \leq j_{max}$ **Do**
  Call PSO
  Calculate: $P_G^u, p_{gap}^u, \omega_o, P_{gap-H}^u, P_{gap-L}^u$
- **Required size of BESS and SC**

  Calculate: B_{max}^u, x, C_{max}^u,
  Call Region reduction iterative search algorithm
- **Optimal size of BESS and SC**

  Calculate: $B_{chg-dcg}^u, BDV^u$
  Call Region reduction iterative search algorithm
Calculate: $P_{GT}^u, E_S^u, C_g^u, F^u$
  $u \leftarrow u + 1$
End While
- **Determination of the optimal solution**

  Generate: $\boldsymbol{SS}$
  Call Minima search algorithm
  Optimal solution

End

VI. SIMULATION RESULTS AND DISCUSSIONS

The first step in our proposed methodology is to find combinations of PV and WT for the reduced search space given in (32). The determination of the combinations is based upon minimization of the cumulative error between load and generation, defined in (23), so that renewable power generation should have better load following. The algorithm

TABLE 3. Economic and technical data of sources.

PV			WT				BES			SC	
FOR_{PV} (—)	C_{inv} ($/kW)	C_{om} ($/kW-yr)	FOR_{WT} (—)	C_{inv} ($/kW)	C_{om} ($/kW-yr)	Life Cycles (No.)	DOD (%)	C_{inv} ($/kWh)	C_{om} ($/kWh-yr)	C_{inv} ($/kWh)	C_{om} ($/kWh-yr)
0.04	2025	16	0.04	2346	33	2500	100	400	10	1000	10

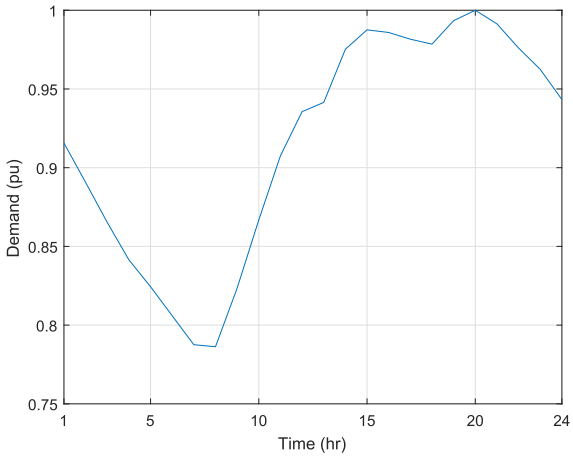

FIGURE 3. Normalized average daily power demand of Dammam of calendar year 2015.

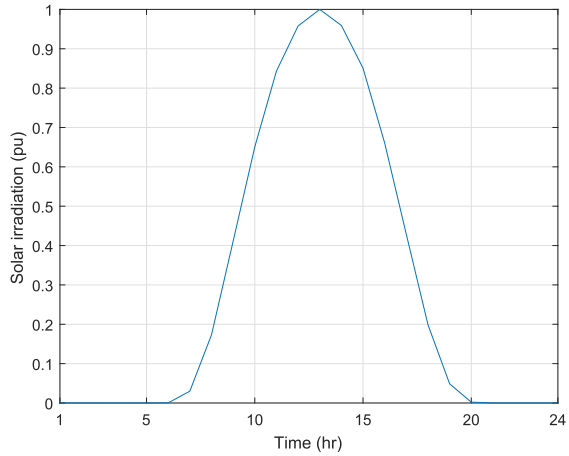

FIGURE 4. Normalized daily average solar irradiation.

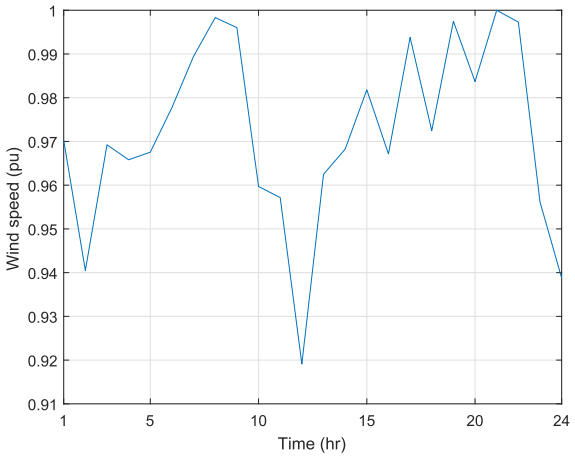

FIGURE 5. Normalized daily average wind speed.

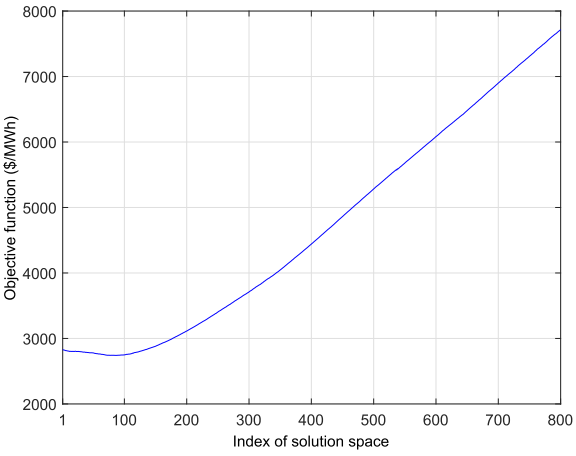

FIGURE 6. Variation in the cost function w.r.t. index of the solution space.

given in Section III-A has selected 800 combinations of PV and WT. As mentioned earlier, RE sources perform effectively when operated with properly sized and suitable type of energy storage. The optimal size of ESS is characterized by both energy storing capacity and maximum power rating. Second step of the strategy is to determine the energy (MWh) and power (MW) capacities of BES system and SC storage. Finally, the optimal combination of PV, WT, BES, and SC is determined based upon three important parameters, i.e., cost, reliability, and GHG emissions. The solution space, as given in (88), is formulated and shown in Fig. 6. It is important to note that for each index of solution space there is a combination of PV, WT, BES, and SC, and optimal combination corresponds to the index with minimum value of objective function. A smaller value of the objective function implies that the energy supplied by the MG is larger, cost per unit of the MG is smaller, GHG emissions are lesser, and emission reduction benefit cost (as defined in (73)) is higher. In the presented case study, the minimum value of cost function appears corresponding to index number 88 which can be seen in Fig. 6.

The optimal capacities of PV, WT, BES, and SC are given in Table 4. The overall cost per unit is USD 0.1552. It is important to note that the cost per unit is the function of many parameters, for example a location with higher correlation between the solar irradiation curve, wind speed curve and load curve would result in further reduction in cost, and our optimized solution will then be more effective and justified.

TABLE 4. Optimal capacities combination.

Source Type	Solar (MW)	Wind (MW)	BES (MWh,MW)	SC (MWh,MW)
Capacity	87	88	48 9.6	4.4 52

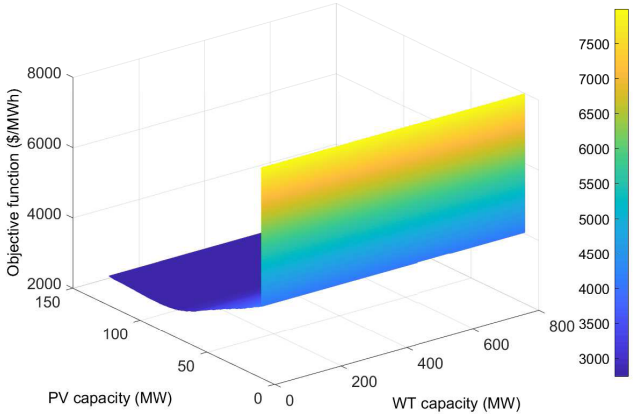

FIGURE 7. Cost function vs different combinations of PV and WT.

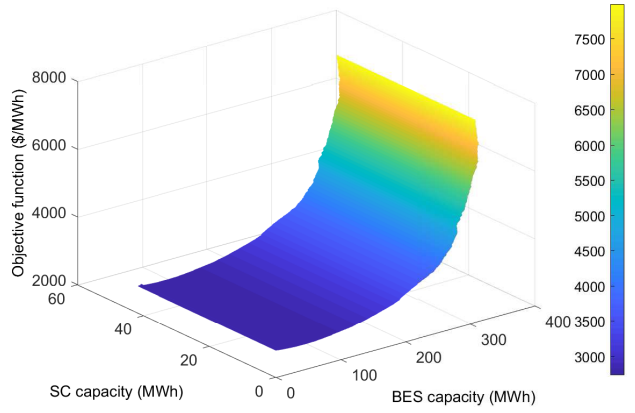

FIGURE 8. Cost function vs different combinations of SC and BES.

In order to get more comprehensible insight in variations of the cost function with RE sources and HESS capacities, the cost function is plotted against the combinations of PV and WT, and SC and BES, that corresponds to each index of solution space shown in Fig. 7 and Fig. 8 respectively. Initially, the installed capacities of both RE sources and HESS are small while values of the cost function are higher because GHG emissions are higher, energy served by the MG is lesser, and ERBC is also small. With the increase in the installed capacities, corresponding values of the cost function decrease because energy supplied by the MG increases which results in lower GHG emissions and increased ERBC. Although, per unit cost also increases with the increase in the installed capacities but its impact on the objective function is non-dominant for moderate capacities. However, for very large capacities, values of the objective function are high because the impact of cost of RE sources and HESS on objective function becomes dominant. Although, for very large capacities

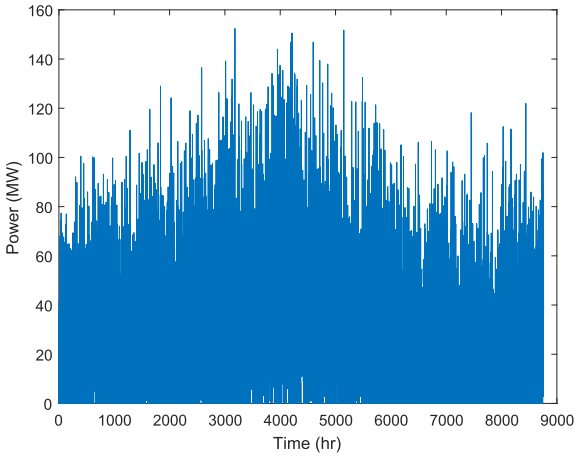

FIGURE 9. Hybrid power generation.

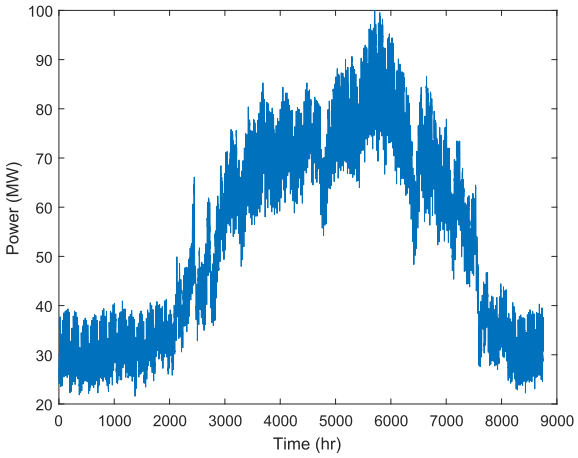

FIGURE 10. Load power demand.

energy supplied by the MG is higher, GHG emissions are lesser and ERBC is also higher but their impact on the cost function is less dominant as compared to the cost of RE sources and HESS. The cost of BES and SC is very high so for larger capacities they have large impact on overall cost of the MG.

The hybrid power generated by optimal PV-WT system and the load power demand are shown in Fig. 9 and Fig. 10 respectively. While the error/gap between the generation and demand is plotted in Fig. 11. This error is required to be supplied to/by energy storage system, which is HESS in our case. The error signal is supplied to/by BES and/or SC depending upon its magnitude and frequency. A histogram of the error signal is presented in Fig. 12 which shows that most of the times the magnitude of error is more than the rated power capacity of BES system. However, most of the times the error signals can be supplied by utilizing the HESS system.

A comparison based upon cost per unit of the MG, GHG emissions, energy served by the MG, and ERBC, between four different possible solutions selected from the solution space, is tabulated in Table 5. Cost per kWh of the MG is

TABLE 5. Comparison between different possible solutions.

Case No.	Index No.	PV Capacity (MW)	WT Capacity (MW)	BES Capacity (MWh)	SC Capacity (MWh)	MG Generation Cost ($/kWh)	GHG Emissions (kt)	Energy Served (GWh)	ERBC (M$)
1	60	100	60	28	3.4	0.28	245	237	5.21
2	**88**	**87**	**88**	**48**	**4.4**	**0.27**	**213**	**269**	**5.90**
3	200	54	200	166	10	0.315	117	362	7.97
4	800	10	800	308	42	0.801	15	463	10.18

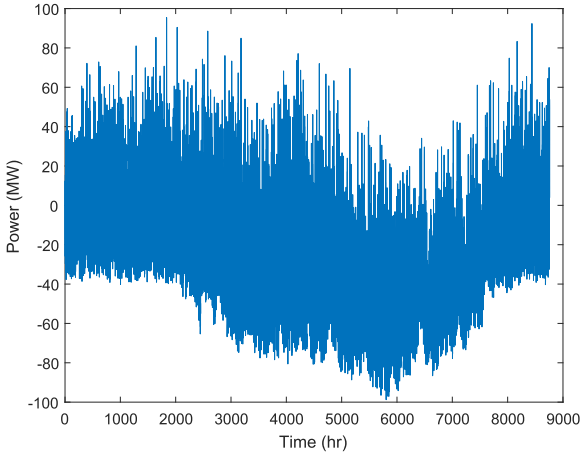

FIGURE 11. Difference in generation and demand.

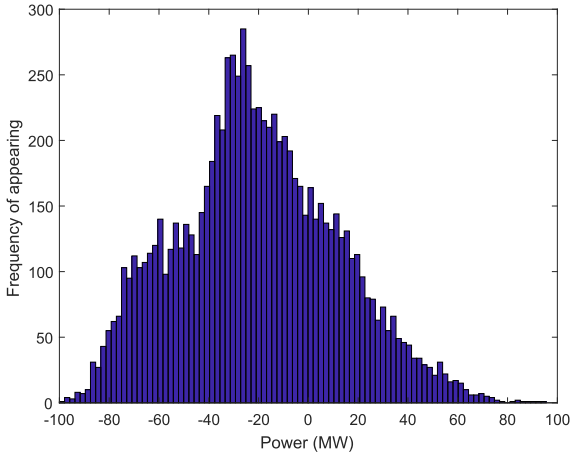

FIGURE 12. Histogram of gap between generation and demand.

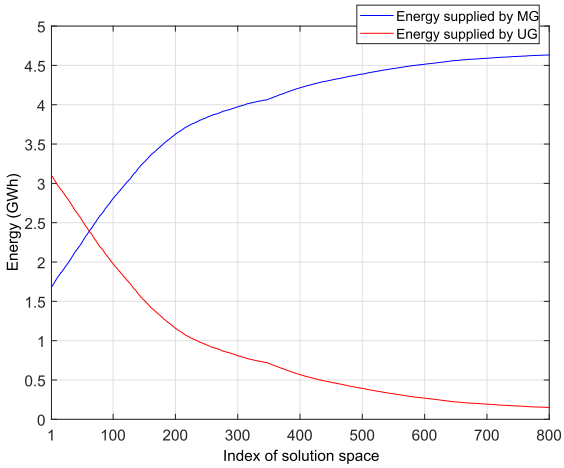

FIGURE 13. Energy share of MG and UG.

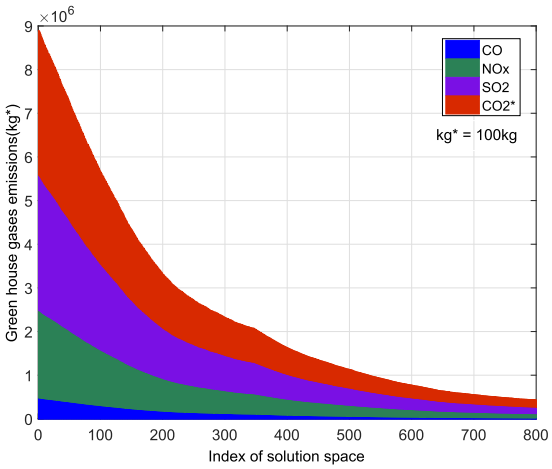

FIGURE 14. Variation in GHG emissions.

minimum for Case number 2 and maximum for Case number 4, since installed capacities in this case are very high. The GHG emissions are minimum for Case number 4 while maximum for Case number 1, and moderate for Case number 2 and 3. Energy served is highest for Case number 4 whilst lowest for Case number 1 and moderate for Case number 2. As the optimal solution is determined based upon the cost, reliability, i.e., energy served, and GHG emissions, Table 5 clearly shows that Case number 2 is optimal.

As mentioned earlier that the output of RE sources is variable, so it may happen during the operation of the MG that output of the RE sources and storage system becomes inadequate to supply the required load demand, during such events, the MG buys power from UG in order to meet the demand. Total energy share supplied by the MG and the UG to fulfill the required load demand is shown in Fig. 13. It can be observed that with the increase in indices the energy supplied by the MG increases while energy supplied by UG decreases. In the beginning, energy supplied by MG increases and energy supplied by utility decreases rapidly and finally both saturates.

The variation in the GHG emissions and ERBC with the indices of solution space are shown in the Figs. 14 and 15

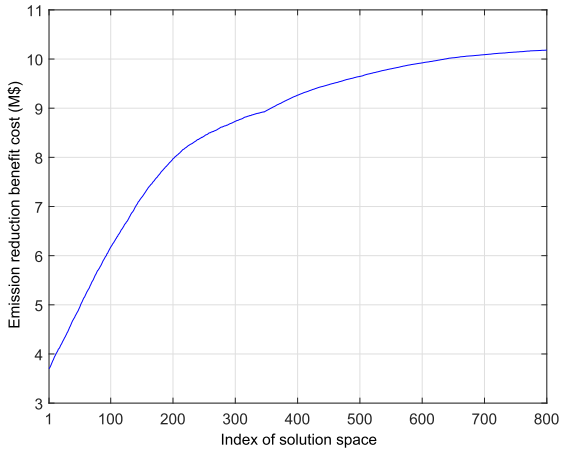

FIGURE 15. Emission reduction benefit cost.

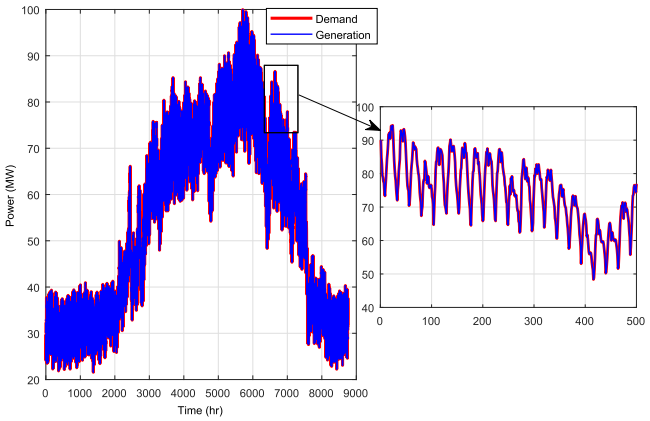

FIGURE 16. Actual demand vs supplied power with optimal system parameters.

respectively. It can be depicted that GHG emissions decrease while ERBC increases with the increase in the index (as overall installed capacities of RE sources and HESS increase with the increase in the index). It can be observed from Fig. 14 that the GHG emissions for the optimal solution are almost 55% less as compared to the conventional generation.

The operation of the MG over a period of one year with the optimal parameters is shown in Fig. 16. It can be observed that the system supplies the required demand effectively. As the system under consideration is grid-connected that is why the generation is always equal to the required load power demand which makes the system highly reliable.

A comparison between the following three case studies is presented in Table 6.

- CASE-I: PV/WT/BES/SC based grid-connected MG.
- CASE-II: PV/WT/BES based grid-connected MG.
- CASE-III: A MG employing conventional generation.

The cost per unit is minimum for CASE-III but it can not be selected as in this case the load demand is served by conventional generation only. The cost per unit of the CASE-I is 0.13% less than that of CASE-II. This can result in savings of about USD 1M per year as compared to CASE-II. So, by employing the HESS instead of BES system, cost per

TABLE 6. Comparison of different case studies.

Index		CASE-I	CASE-II	CASE-III
WT (MW)		88	88	0.0
PV (MW)		87	87	0.0
BES (MWh)		48	49	0.0
SC (MWh)		4.4	0.0	0.0
Energy (GWh)	MG	269	266	0.0
	Utility	209	212	478
Emissions (T)	CO	357	362	817
	CO_2	230544	233854	527274
	NOx	1488	1510	3404
	SO_2	2302	2335	5265
Cost ($/MWh)		155.2	155.4	100
ERBC (M$)		5.9	5.8	0.0

unit decreases which results in considerable savings. This decrease in the cost is due to the fact that the SC prolongs the lifespan of BES system. The clean energy (energy from MG) supplied by the CASE-I is more than that of CASE-II. Similarly, the emissions are minimum for CASE-I and maximum for CASE-III. The emissions for CASE-I are approximately 55% less than that of CASE-III. These less GHG emissions also result in considerable savings in terms of ERBC and it can be seen from the Table 6 that the ERBC is maximum for CASE-I. So, the HESS is not only economical but also more reliable and cleaner as compared to BES.

VII. CONCLUSION

This paper has presented a methodology for joint capacity optimization of hybrid renewable power generation system and energy storage in the context of a grid-connected microgrid (MG). The hybrid generation system is comprised of solar photovoltaic (PV) and wind turbine (WT) and hybrid energy storage system (HESS) is composed of battery energy storage (BES) system and supercapacitor (SC) technology. The combined optimization exploits the benefits of both hybrid power generation and HESS. The proposed strategy is primarily based upon a few important factors associated with a MG system such as cost minimization, greenhouse gases (GHG) emissions reduction, higher emission reduction benefit cost (ERBC), and higher reliability. The optimization problem has been formulated and solved in a piece-wise fashion to decrease the complexity and computational time.

The proposed methodology has been tested using real residential power demand, solar irradiation and wind speed data. The resulted optimal solution is economical, has higher reliability and lesser GHG emissions when compared with other possible solutions. It has also been shown that when the MG is operated with optimal parameters it serves the demand effectively. Moreover, a comparison between three case studies, i.e., PV/WT/BES/SC, PV/WT/BES, and conventional generation has also been presented. It has been observed that the topology, PV/WT/BES/SC, resulted in the optimal choice as there are multiple benefits associated with hybrid

BES-SC energy storage system. It is an economical and reliable solution because the use of SC in conjunction with BES prolongs the BES lifespan, and supplies the demand more effectively and efficiently. In addition, it results in least GHG emissions thus increasing ERBC which makes the overall system more economical and eco-friendly.

For future research, a detailed load analysis considering different types of loads including controllable and uncontrollable loads, and load shifting will be performed to determine an optimum combination of RE sources along with conventional generation that fulfills the load effectively and economically. Furthermore, uncertainty associated with the availability of RE sources and degradation of battery energy storage will also be considered for more realistic results.

ACKNOWLEDGMENT

The authors would like to thank the Research Institute (RI) at KFUPM and Saudi Electricity Company (SEC) for providing the time series data of solar irradiation, wind speed data and residential load data.

REFERENCES

[1] F. Blaabjerg, R. Teodorescu, M. Liserre, and A. V. Timbus, "Overview of control and grid synchronization for distributed power generation systems," *IEEE Trans. Ind. Electron.*, vol. 53, no. 5, pp. 1398–1409, Oct. 2006.

[2] E. Kuznetsova, C. Ruiz, Y.-F. Li, and E. Zio, "Analysis of robust optimization for decentralized microgrid energy management under uncertainty," *Int. J. Electr. Power Energy Syst.*, vol. 64, pp. 815–832, Jan. 2015.

[3] A. Kyritsis *et al.*, "Evolution of PV systems in Greece and review of applicable solutions for higher penetration levels," *Renew. Energy*, vol. 109, pp. 487–499, Aug. 2017.

[4] H. T. Le and T. Q. Nguyen, "Sizing energy storage systems for wind power firming: An analytical approach and a cost-benefit analysis," in *Proc. IEEE Power Energy Soc. Gen. Meet.-Convers. Del. Electr. Energy 21st Century*, Jul. 2008, pp. 1–8.

[5] P. Denholm and R. M. Margolis, "Evaluating the limits of solar photovoltaics (PV) in electric power systems utilizing energy storage and other enabling technologies," *Energy Policy*, vol. 35, no. 9, pp. 4424–4433, 2007.

[6] B. Yang *et al.*, "On the use of energy storage technologies for regulation services in electric power systems with significant penetration of wind energy," in *Proc. IEEE 5th Int. Conf. Eur. Electr. Market*, May 2008, pp. 1–6.

[7] A. Khatamianfar, M. Khalid, A. V. Savkin, and V. G. Agelidis, "Improving wind farm dispatch in the australian electricity market with battery energy storage using model predictive control," *IEEE Trans. Sustain. Energy*, vol. 4, no. 3, pp. 745–755, Jul. 2013.

[8] M. Khalid and A. V. Savkin, "A model predictive control approach to the problem of wind power smoothing with controlled battery storage," *Renew. Energy*, vol. 35, no. 7, pp. 1520–1526, 2010.

[9] M. Aneke and M. Wang, "Energy storage technologies and real life applications—A state of the art review," *Appl. Energy*, vol. 179, pp. 350–377, Oct. 2016.

[10] A. V. Savkin, M. Khalid, and V. G. Agelidis, "A constrained monotonic charging/discharging strategy for optimal capacity of battery energy storage supporting wind farms," *IEEE Trans. Sustain. Energy*, vol. 7, no. 3, pp. 1224–1231, Jul. 2016.

[11] M. Khalid, A. Ahmadi, A. V. Savkin, and V. G. Agelidis, "Minimizing the energy cost for microgrids integrated with renewable energy resources and conventional generation using controlled battery energy storage," *Renew. Energy*, vol. 97, pp. 646–655, Nov. 2016.

[12] T. Ma, H. Yang, and L. Lu, "Development of hybrid battery–supercapacitor energy storage for remote area renewable energy systems," *Appl. Energy*, vol. 153, pp. 56–62, Sep. 2015.

[13] A. Schneuwly. (2006). "High reliability power backup with advanced energy storage." Maxwell Technol. San Diego, CA, USA. White Paper. Accessed: Nov. 11, 2017. [Online] https://www.tecategroup.com/white_papers/200904_WhitePaper_EDNEurope_ASchneuwly.pdf

[14] Q. Xu *et al.*, "A decentralized dynamic power sharing strategy for hybrid energy storage system in autonomous DC microgrid," *IEEE Trans. Ind. Electron.*, vol. 64, no. 7, pp. 5930–5941, Jul. 2017.

[15] J. Shen and A. Khaligh, "A supervisory energy management control strategy in a battery/ultracapacitor hybrid energy storage system," *IEEE Trans. Transport. Electrific.*, vol. 1, no. 3, pp. 223–231, Oct. 2015.

[16] Y. Liu, W. Du, L. Xiao, H. Wang, S. Bu, and J. Cao, "Sizing a hybrid energy storage system for maintaining power balance of an isolated system with high penetration of wind generation," *IEEE Trans. Power Syst.*, vol. 31, no. 4, pp. 3267–3275, Jul. 2016.

[17] S. Zhang, R. Xiong, and J. Cao, "Battery durability and longevity based power management for plug-in hybrid electric vehicle with hybrid energy storage system," *Appl. Energy*, vol. 179, pp. 316–328, Oct. 2016.

[18] J. M. Blanes, R. Gutiérrez, A. Garrigós, J. L. Lizán, and J. M. Cuadrado, "Electric vehicle battery life extension using ultracapacitors and an FPGA controlled interleaved buck–boost converter," *IEEE Trans. Power Electron.*, vol. 28, no. 12, pp. 5940–5948, Dec. 2013.

[19] B. Hredzak, V. G. Agelidis, and M. Jang, "A model predictive control system for a hybrid battery-ultracapacitor power source," *IEEE Trans. Power Electron.*, vol. 29, no. 3, pp. 1469–1479, Mar. 2014.

[20] H. Lotfi and A. Khodaei, "Hybrid AC/DC microgrid planning," *Energy*, vol. 118, pp. 37–46, Jan. 2017.

[21] A. S. O. Ogunjuyigbe, T. R. Ayodele, and O. A. Akinola, "Optimal allocation and sizing of PV/Wind/Split-diesel/Battery hybrid energy system for minimizing life cycle cost, carbon emission and dump energy of remote residential building," *Appl. Energy*, vol. 171, pp. 153–171, Jun. 2016.

[22] R. Hosseinalizadeh, H. Shakouri, M. S. Amalnick, and P. Taghipour, "Economic sizing of a hybrid (PV–WT–FC) renewable energy system (HRES) for stand-alone usages by an optimization-simulation model: Case study of Iran," *Renew. Sustain. Energy Rev.*, vol. 54, pp. 139–150, Feb. 2016.

[23] P. Yang and A. Nehorai, "Joint optimization of hybrid energy storage and generation capacity with renewable energy," *IEEE Trans. Smart Grid*, vol. 5, no. 4, pp. 1566–1574, Jul. 2014.

[24] T. Dragičević, H. Pandžić, D. Škrlec, I. Kuzle, J. M. Guerrero, and D. S. Kirschen, "Capacity optimization of renewable energy sources and battery storage in an autonomous telecommunication facility," *IEEE Trans. Sustain. Energy*, vol. 5, no. 4, pp. 1367–1378, Oct. 2014.

[25] M. Sharafi and T. Y. ELMekkawy, "Multi-objective optimal design of hybrid renewable energy systems using PSO-simulation based approach," *Renew. Energy*, vol. 68, pp. 67–79, Aug. 2014.

[26] L. Xu, X. Ruan, C. Mao, B. Zhang, and Y. Luo, "An improved optimal sizing method for wind-solar-battery hybrid power system," *IEEE Trans. Sustain. Energy*, vol. 4, no. 3, pp. 774–785, Jul. 2013.

[27] E. E. Sfikas, Y. A. Katsigiannis, and P. S. Georgilakis, "Simultaneous capacity optimization of distributed generation and storage in medium voltage microgrids," *Int. J. Electr. Power Energy Syst.*, vol. 67, pp. 101–113, May 2015.

[28] J. Zhu *et al.*, "Learning automata-based methodology for optimal allocation of renewable distributed generation considering network reconfiguration," *IEEE Access*, vol. 5, pp. 14275–14288, 2017.

[29] J. Chen *et al.*, "Optimal sizing for grid-tied microgrids with consideration of joint optimization of planning and operation," *IEEE Trans. Sustain. Energy*, to be published, doi: 10.1109/TSTE.2017.2724583.

[30] R. Atia and N. Yamada, "Sizing and analysis of renewable energy and battery systems in residential microgrids," *IEEE Trans. Smart Grid*, vol. 7, no. 3, pp. 1204–1213, May 2016.

[31] C. S. Lai and M. D. McCulloch, "Sizing of stand-alone solar PV and storage system with anaerobic digestion biogas power plants," *IEEE Trans. Ind. Electron.*, vol. 64, no. 3, pp. 2112–2121, Mar. 2017.

[32] A. Askarzadeh, "Electrical power generation by an optimised autonomous PV/wind/tidal/battery system," *IET Renew. Power Generat.*, vol. 11, no. 1, pp. 152–164, 2016.

[33] Y. A. Katsigiannis, P. S. Georgilakis, and E. S. Karapidakis, "Hybrid simulated annealing–tabu search method for optimal sizing of autonomous power systems with renewables," *IEEE Trans. Sustain. Energy*, vol. 3, no. 3, pp. 330–338, Jul. 2012.

[34] T. Zhou and W. Sun, "Optimization of battery–supercapacitor hybrid energy storage station in wind/solar generation system," *IEEE Trans. Sustain. Energy*, vol. 5, no. 2, pp. 408–415, Apr. 2014.

[35] A. Abbassi, M. A. Dami, and M. Jemli, "A statistical approach for hybrid energy storage system sizing based on capacity distributions in an autonomous PV/Wind power generation system," *Renew. Energy*, vol. 103, pp. 81–93, Apr. 2017.
[36] A. Arabali, M. Ghofrani, M. Etezadi-Amoli, and M. S. Fadali, "Stochastic performance assessment and sizing for a hybrid power system of solar/wind/energy storage," *IEEE Trans. Sustain. Energy*, vol. 5, no. 2, pp. 363–371, Apr. 2014.
[37] S. X. Chen, H. B. Gooi, and M. Q. Wang, "Sizing of energy storage for microgrids," *IEEE Trans. Smart Grid*, vol. 3, no. 1, pp. 142–151, Mar. 2012.
[38] S. Rehman, T. O. Halawani, and T. Husain, "Weibull parameters for wind speed distribution in Saudi Arabia," *Solar Energy*, vol. 53, no. 6, pp. 473–479, 1994.

UMER AKRAM (S'16) received the B.Sc. degree (Hons.) in electrical engineering from the COMSATS Institute of Information Technology, Abbottabad, Pakistan, in 2013. He is currently pursuing the M.S. degree in electrical engineering from the King Fahd University of Petroleum and Minerals, Saudi Arabia. His current research interests include modern power system planning, operation and design, optimization and control of distributed energy resources, renewable energy, and energy storage systems.

MUHAMMAD KHALID (M'09) received the Ph.D. degree in electrical engineering from the School of Electrical Engineering and Telecommunications (EE&T), University of New South Wales (UNSW), Sydney, Australia, in 2011. He was a Post-Doctoral Research Fellow for three years and then he continued as a Senior Research Associate with the School of EE&T, Australian Energy Research Institute, UNSW, for another two years. He is currently serving as an Assistant Professor for the Electrical Engineering Department, King Fahd University of Petroleum and Minerals, Dhahran, Saudi Arabia. He has authored/co-authored several journal and conference papers in the field of control and optimization for renewable power systems. His current research interests include the optimization and control of battery energy storage systems for large-scale grid-connected renewable power plants (particularly wind and solar), distributed power generation and dispatch, hybrid energy storage, EVs, and smart grids. He was a recipient of a highly competitive post-doctoral writing fellowship from UNSW in 2010. He has been a reviewer for numerous international journals and conferences.

SAIFULLAH SHAFIQ received the B.Sc. degree in electrical engineering from the University of Engineering and Technology, Lahore, Pakistan, in 2014. He is currently pursuing the M.S. degree in electrical engineering from the King Fahd University of Petroleum and Minerals, Dhahran, Saudi Arabia. His current research interests include power system planning, renewable energy resources, electric vehicles, and power electronics.